



ISSN:2230-9926

Available online at <http://www.journalijdr.com>

IJDR

International Journal of
DEVELOPMENT RESEARCH

International Journal of Development Research
Vol. 4, Issue, 2, pp. 244-247, February, 2014

Full Length Research Article

MODELING IONIZATION EFFECTS IN A BNCT FIELD

*Mohammadi, S. and Shaheidari, R.

Department of Physics, Payame Noor University, PO BOX 19395-3697 Tehran, Iran

ARTICLE INFO

Article History:

Received 20th November, 2013

Received in revised form

05th December, 2013

Accepted 23rd January, 2014

Published online 21st February, 2014

Key words:

BNCT;

Ionization effects;

Lithium; Alpha;

Protons; Healthy tissue

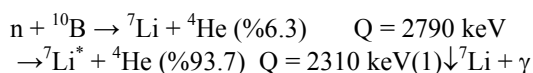
ABSTRACT

The Ionization effects of charged particles produced in neutron interactions for Boron Neutron Capture Therapy (BNCT) are considered here using SRIM Monte Carlo Code. The estimated values of these effects in a Plexiglas acrylic phantom are shown to agree well with the available experimental values in high Boron concentration areas. As expected, the ionization effects from lithium and alpha particles are significant. In the low Boron areas, proton ionization makes an important contribution and its effect on healthy tissue should not be ignored.

Copyright © 2013 Mohammadi, S. and Shaheidari, R. This is an open access article distributed under the Creative Commons Attribution License, which permits unrestricted use, distribution, and reproduction in any medium, provided the original work is properly cited.

INTRODUCTION

In Boron Neutron Capture Therapy (BNCT), a tumor is irradiated by thermal neutrons (Medina *et al.*, 2005). Boron atoms are introduced to the tumor and gather in the cancer cells. Higher thermal neutrons interaction cross-section of Boron causes strong impressive ionization damage to the tumor. Boron -10 thermal neutron capture results in the following nuclear reactions:



The produced lithium and alpha particles have a high Linear Energy Transfer (LET); they deposit their energy within ranges of 4.1 and 7.7 μm respectively, which are comparable to a typical cell dimension. The energy deposition depends strongly on spatial deposition of the B-10 nuclei and in concentrations in the tumor (Tanaka *et al.*, 2005). In addition to the absorbed dose due to B-10 neutron capture, many other dose components are present. Protons are recoil products from the interaction of both fast and epithermal neutrons with hydrogen nuclei in $n + p \rightarrow n' + p'$ interaction. Carbon recoil products come from the interaction ${}^{12}\text{C} (n, n){}^{12}\text{C}$. In addition

to the above interaction, neutrons have another interactive mode with atomic nuclei in matter. The interaction of epithermal neutrons with matter in the BNCT field can result in protons, carbon and oxygen ions as products. The charged particles produced move in matter and ionized it, deposit their energy and eventually have remarkable destructive effects. In this research, the ionization effects of all particles produced in a Plexiglas acrylic phantom are investigated. The unwanted ionization effects are compared with the ionization effects caused by Lithium ions and alpha particles are considered to be basic ionizing particles in BNCT. We study charged particle tracks in matter by using The Stopping and Range of Ions in Matter (SRIM) code (Ziegler and Biersack, 2003). The precision of a Monte Carlo approach for computing charge particle trajectories in matter depends mainly on the precision of the calculation of the stopping power properties of the matter. A direct calculation of charge particle stopping powers in matter is practically possible by using the transport of ions in matter and by using SRIM computer code. It is proved that the SRIM Monte Carlo modeling could adequately predict the dose to tissue in BNCT treatment.

MATERIALS AND METHODS

To simulate a neutron field and charged particle trajectories, we use a Plexiglas acrylic phantom ($\text{C}_4\text{H}_6\text{O}_2$, $\rho = 1.17 \text{ g cm}^{-3}$) in considering BNCT and simulate charge particle tracks by Monte Carlo computing using the SRIM computer code. This

*Corresponding author: Mohammadi, S.

Department of Physics, Payame Noor University, PO BOX 19395-3697 Tehran, Iran

phantom is used to be able to compare the obtained Monte Carlo calculations with available experimental values. Epithermal neutrons have different modes of interaction with tissue being considered here. Elastic scattering can take place upon interaction with hydrogen, carbon and oxygen nuclei. Elastic scattering cross-sections for these interactions are shown in Figure 1 (Neutron Cross Section Lab.). To be able to evaluate the effect of charged particles produced from neutron interactions, the initial energies of particles are needed. Recoiled protons in the elastic scattering of epithermal neutrons by a hydrogen nucleus have the same energy as the incident nucleus; they move in matter and ionize it. These calculations are done by using SRIM computer code. Recoiled carbon ions in ^{12}C (n, n) ^{12}C .

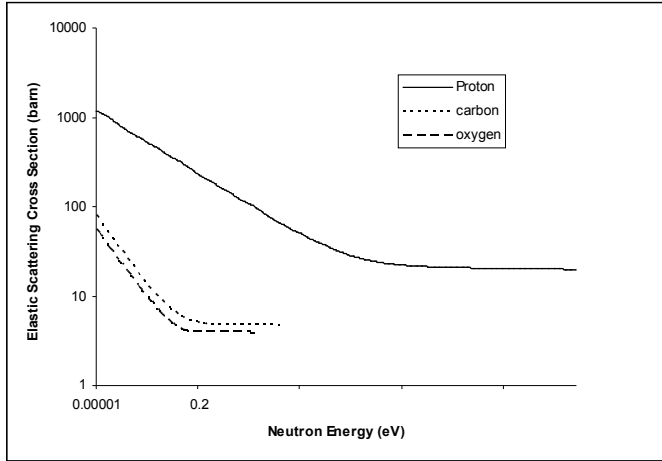


Figure 1. Elastic scattering cross-section variation

and oxygen ions in ^{16}O (n, n) ^{16}O elastic interactions have average initial energies of 2.84 keV and 2.215 keV, respectively. Furthermore, the thermal neutrons capture by B-10, results in alpha particles and lithium ions with 1470 and 840 keV initial energies, respectively. Several useful statistical quantities can be defined to estimate the statistical accuracy of the results obtained by SRIM code. Straggling range (σ), Skewness (γ) and Kurtosis (β) are defined as (Ziegler, 2003):

$$\sigma = \langle (\Delta)^2 \rangle^{1/2} \quad (2)$$

$$\gamma = \langle \Delta x^3 \rangle / \langle \Delta x^2 \rangle^{3/2} \quad (3)$$

$$\beta = \langle \Delta x^4 \rangle / \langle \Delta x^2 \rangle^2 \quad (4)$$

In this way, straggling range is the square root of the variance, which itself is the second moment distribution of the range. The skewness tells whether the peak is skewed towards the surface (negative values) or away from the surface (positive values). Negative skewness indicates that the most probable depth (the peak position) is greater than the mean depth, and positive values indicate the reverse. Kurtosis indicates the extent of the distribution tails, with a value of 3.0 indicating a Gaussian distribution. Since both the shallow and deep tails contribute, no simple rule indicates what a deviation from 3.0 means for the ion distribution. In general, values from 0 to 3 indicate abbreviated tails, and values above 3 indicate broad tails (Ziegler, 2003).

RESULTS AND DISCUSSION

In using Plexiglas phantom, the energy loss versus depth due to ionization by alpha particles and lithium ions produced by

the capture of thermal neutrons in Boron-10 are shown in Figure 2. The effects of recoiled particles in this ionization process can be neglected; they are not much in evidence in the Figure. The same curves for carbon and oxygen ions are shown in Figures 3 and 4 respectively. The effects of recoiled particles in these ionization interactions are comparable to those of the direct ionization effects by carbon and oxygen ions. Furthermore, the energy loss versus depth in Plexiglas due to ionization for protons and recoils are shown in Figure 5. It can be seen that ionization effects due to the recoiled particles can be neglected.

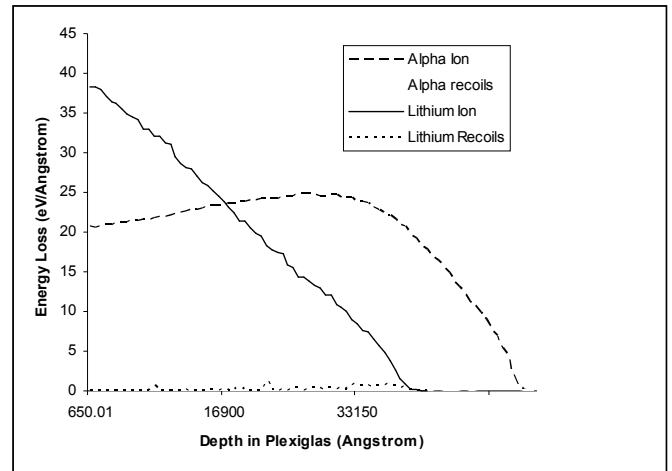


Figure 2. Lithium ions and Alpha particle energy loss

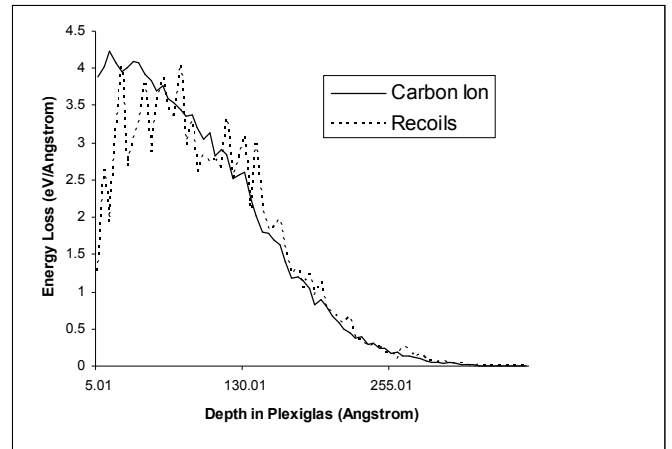


Figure 3. Carbon ions and recoils energy loss

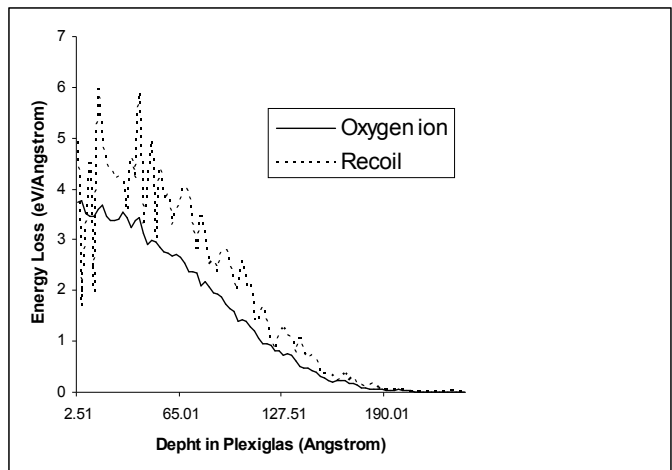


Figure 4. Oxygen ions and recoils energy loss

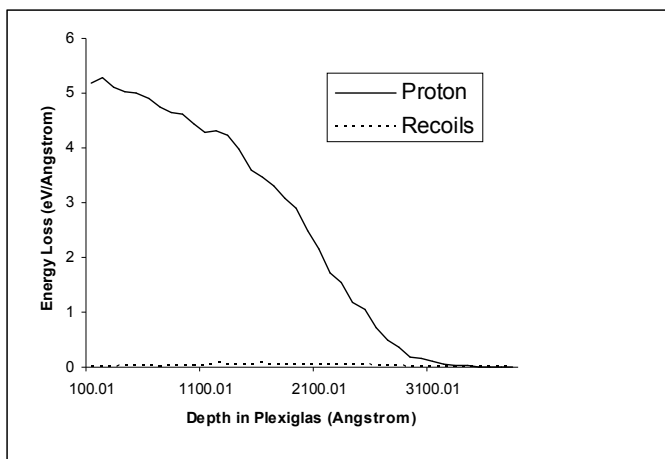


Figure 5. Proton and recoils energy loss

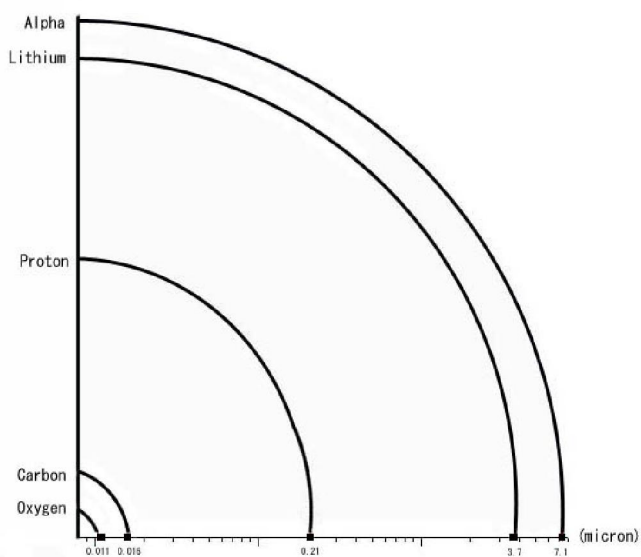


Figure 6. Comparing radius of spheres

The calculated ion ranges for the various ions are shown in Figure 6. It can be seen that the alpha particles produced from thermal neutron capture by boron have the largest ion range (from generation to stop location), in comparison to the other particles produced. SRIM results for the calculated ion initial energy, energy loss and defined statistical quantities for various ions are shown in Table 1.

Table 1. SRIM results for energy and statistical quantities

	Proton	C-12	O-16	He	Li-7
Ion Initial Energy (keV)	10	2.84	2.21	1470	840
Energy Loss in Range (keV)	9.172	0.566	0.322	1451	803.3
Recoil Energy Loss (keV)	0.001	0.529	0.426	0.003	0.014
Struggle (µm)	0.050	0.006	0.004	0.164	0.203
Skewness	-0.55	0.10	0.12	-2.69	-3.01
Kurtosis	4.06	2.61	2.59	25.76	30.66

Each alpha particle produced can ionize the matter in a sphere concentrated on the generation location with a radius equal to 7.120 µm. From its initial energy (1470 keV), it can deposit about 98.6% (1450 keV) for ionizing media. Furthermore, it is obvious from table 1 that oxygen ions have the least range in Plexiglas relative to other particles. Every oxygen ion from its initial energy (2.21 keV) deposits 0.332 keV, namely 13.57

per cent, for direct ionization and 0.426 keV (18 per cent) for indirect secondary ionization. Ionization energy is saved in a sphere of radius 0.011 µm centered on the generation location. The remaining ion energy is spent for increasing thermal vibrations of atoms in media. In order to be able to compare the straggling range for ions, we define parameter η as (Ziegler and Biersack, 2003):

$$\eta = \frac{\sigma}{x} = \frac{\langle(\Delta x)^2\rangle^{1/2}}{x} \quad (5)$$

where η is a criterion for uncertainty concerning the frontier of sphere. It can be seen from table 1 that the oxygen and carbon ions have the least range of straggling and lithium ions and alpha particles from Boron neutron capture have the largest straggling. But, the defined η indicates that uncertainty for lithium ions and alpha particles is small and for other ions becomes larger. The skewness values for alpha particles, protons and lithium ions are negative, indicating that their peak is skewed towards the surface. Carbon and oxygen ions have positive skewness indicating peak is away from the surface. Therefore, carbon and oxygen ions with high probability will stop before reaching their mean stopping location, while alpha particles, protons and lithium ions will more likely stop after their mean stopping location. Kurtosis values for carbon and oxygen ions are in the range from 0 to 3 and therefore have abbreviated tails; alpha particles, protons and lithium ions have a kurtosis value above 3 and therefore have broad tails. Kurtosis values for oxygen, carbon and protons indicate a distribution similar to a Gaussian shape. An experimental evaluation of the beam quality of the clinical BNCT neutron field at Kyoto university reactor, based on a microdosimetric technique was studied by Endo, *et al.* (2004). It was shown that the estimated relative contributions of the neutron dose on proton, alpha particles and carbon ions are 0.9, 0.07 and 0.03, respectively. In this evaluation, the effects of oxygen and lithium ions were not considered.

In the mentioned experimental evaluation, a Tissue Equivalent Proportional Counter (TEPC) and a Carbon Walled Proportional Counter (CWPC) were used for measurements and the results obtained compared. The TEPC and CWPC were filled by methane-based tissue equivalent and CO₂ gases respectively, at a certain pressure (Endo *et al.*, 2004). As CWPC does not contain hydrogen neither in the wall nor in filling gas, the recoiled carbons from elastic scattering produced in tissue can be simulated. In order to be able to compare experimental results to our calculated values using SRIM code, the per cent of ionization effects by protons, carbon ions and alpha particles are calculated and given in Table 2. It can be seen that there is a good agreement for protons, but the relative contribution to neutron dose from alpha particles and carbon ions in SRIM calculation are equal. It is also obvious that ionization effects due to the other particles are insignificant when compared with the effects due to lithium ions and alpha particles. Because of the low concentrations of boron in matter as compared with oxygen, hydrogen and carbon, clearly the probability of alpha or lithium productions is very small in comparison to protons and recoiled oxygen and carbon atoms. But, in fact the ionization from these particles can have serious effects and damages in the amount of dose absorbed. For example, in a typical experiment, if the boron concentration is considered to be

2000 ppm (Tanaka *et al.*, 2005), and we assume the probability of interaction is proportional to particle concentration and neutron interaction cross section in 10 keV (Neutron Cross Section Lab.), the calculated per cent of ionization effects of these particles is shown in Table 3. It can be seen that the ionization effects depend strongly on protons and so the dose amount needs to be kept low. Furthermore, the ionization effects due to carbon and oxygen ions are not ignorable. In BNCT, we can control the boron concentration dose in the tumor relative to healthy tissue, but we should not ignore the effect of protons on health tissues.

Table 2. Per cent of ionization effects due to carbon, proton and alpha

	Carbon	Proton	Alpha
This Work	0.055	0.89	0.055
Reference (8)	0.03	0.9	0.07

Table 3. Per cent of ionization effects due all particles

Carbon	Proton	Oxygen	Lithium	Alpha
11.17	51.31	4.14	11.89	21.49

Conclusions

For protons, carbon ions, alpha particles, lithium and oxygen ions produced in BNCT, their range and other important statistical parameters were calculated using the SRIM Monte Carlo code. The ionization effects due to these particles were estimated in a Plexiglas acrylic phantom and compared with the available experimental values, showing a good agreement.

It is also shown that ionization effects due to the recoiled charged particles compared to the effects due to lithium ions and alpha particles are insignificant. Having considered the Boron concentration and relevant neutron beam cross sections, it is shown that the ionization effect of protons on the healthy tissues is more than the other by-products and should not be ignored. Finally, it is proved that the used SRIM Monte Carlo modeling is adequate to predict the dose to tissue in BNCT treatments.

REFERENCES

Medina D C, Li X, and Springer Jr C S, 2005. Pharmacothermodynamics of deuterium-induced edema in living rat brain via 1H2O MRI: implications for boron neutron capture therapy of malignant brain, tumors, *Phys. Med. Biol.* 50.

Tanaka K, Kobayashi T, Bengua G, Nakagawa Y, Endo Sand and Hoshi M, 2005. Characteristics of boron-dose enhancer dependent on dose protocol and 10B concentration for BNCT using near-threshold ⁷Li(p, n)⁷Be direct neutrons, *Phys. Med. Biol.* 50.

Ziegler J F, Biersack J P, 2003. The Stopping and Range of Ions in Matter, *SRIM-2003.26*.

Neutron Cross Section Lab., available in <http://www.nea.fr/janis>

Ziegler J F, 2003. The Stopping and Range of Ions in Matter, *Instruction Manual*, version 96.xx.

Endo S, Onizuka Y, Ishikawa M, Takada M, Sakurai Y, Kobayashi T, Tanaka K, Hoshi M and Shizuma K, 2004. Microdosimetry of neutron field for boron neutron capture therapy at Kyoto university reactor, *Radiation Protection Dosimetry*, 110.
